THE JOURNAL OF PHYSICAL CHEMISTRY C

pubs.acs.org/JPCC Article

Ultrafast Triplet Pair Separation and Triplet Trapping following Singlet Fission in Amorphous Pentacene Films

Published as part of The Journal of Physical Chemistry virtual special issue "Josef Michl Festschrift".

Kyle T. Munson, Jianing Gan, Christopher Grieco, Grayson S. Doucette, John E. Anthony, and John B. Asbury*

Cite This: *J. Phys. Chem. C* 2020, 124, 23567−23578 Read Online

ACCESS | Metrics & More | Article Recommendations | Supporting Information

ABSTRACT: Ultrafast infrared and electronic spectroscopy are used to examine the dynamics of triplet pair separation following singlet fission in amorphous and crystalline films of the model singlet fission chromophore, 6,13-bis(triisopropylsilylethynyl)-pentacene (TIPS-Pn). Probing of correlated triplet pair intermediates directly through their unique vibrational frequencies and infrared electronic transitions and indirectly through their visible triplet absorptions reveals that triplet pair separation occurs on similar picosecond time scales in both amorphous and crystalline films despite their markedly different average intermolecular coupling strengths. Although triplet pair separation occurs on similar time scales in both environments, measurements of diffusion-controlled triplet−triplet annihilation reveal that the diffusivity of triplet excited states is an order of magnitude lower in amorphous films. The data reveal the presence of sparse triplet traps in the amorphous environment that inhibit the transport of triplet excitons in comparison to crystalline films. These observations inform recent efforts to develop disordered and polymeric singlet fission sensitizers that contain amorphous regions. In particular, the data suggest that it may be possible to nanostructure amorphous or polymeric singlet fission sensitizers to allow ultrafast triplet pair separation and harvesting in photovoltaic and light-emitting applications despite their low triplet exciton diffusivity.

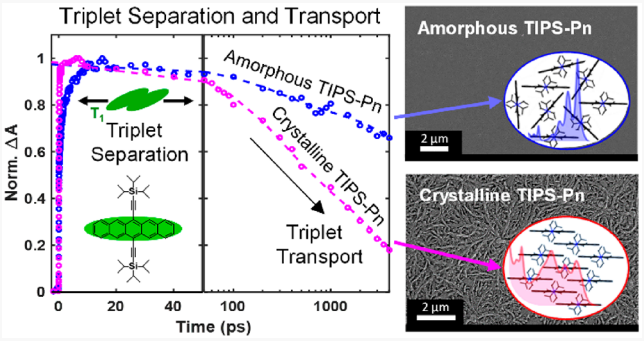

INTRODUCTION

Singlet fission is a multiple exciton generation process that occurs in some conjugated organic molecules[1] and polymers[2,3] wherein the fission of a singlet exciton produces two triplet excitons. Contemporary work on singlet fission suggests that the process may involve multiple intermediates described by the expression

$$S_1S_0 \rightleftharpoons [^1(TT) \rightleftharpoons {}^1(T...T)] \rightleftharpoons T_1 + T_1 \quad (1)$$

where S_1S_0 represents one molecule in its first excited singlet state neighboring a molecule in its ground state, $^1(TT)$ represents an intermediate species called a correlated triplet pair, $^1(T...T)$ is a spatially separated but still spin correlated triplet pair, and T_1 is an independent triplet exciton.[4−6] Spectroscopic studies of model systems such as 6,13-bis(triisopropylsilylethynyl)pentacene (TIPS-Pn) have shown that the formation of correlated triplet pair $^1(TT)$ intermediates can occur rapidly and with high quantum yield[7−9] due to this step being spin-allowed.[7]

Recent studies of crystalline TIPS-Pn films have demonstrated that the initial separation of $^1(TT)$ intermediates in these materials is efficient and can occur on the few picoseconds time scale.[10,11] Likewise, efficient triplet pair separation also has been observed in the crystalline forms of other singlet fission materials, such as crystalline rubrene.[12] In general, a high rate of $^1(TT)$ separation is often viewed as desirable because this can facilitate favorable competition with excited state relaxation pathways that would otherwise reduce the yield of multiplied triplet excitons.[6] As a result, several studies have suggested that crystalline materials should be targeted for next-generation singlet fission sensitized photovoltaics, for example.[10,13,14]

The $^1(TT)$ intermediates produced in the first step of singlet fission in pentacene derivatives are believed to spatially separate to form separated but still spin correlated

Received: August 31, 2020
Revised: October 4, 2020
Published: October 14, 2020

https://dx.doi.org/10.1021/acs.jpcc.0c07920
J. Phys. Chem. C 2020, 124, 23567−23578

intermediates ^{1}(T...T) before undergoing spin decoherence to form two independent triplet excitons $2T_1$ (eq 1).[15,16] In principle, these triplet excitons can then undergo energy or charge transfer in a photovoltaic device,[17−20] enhancing the power conversion efficiencies of existing photovoltaic technologies by reduction of their thermalization losses from higher energy photons.[21] Additionally, singlet fission materials have also been explored to enhance the efficiencies of organic light-emitting devices.[22]

Although the yield of triplet exciton multiplication has been reported to be nearly 200% from spectroscopic measurements,[1,23−25] the reported enhancements in the performance of photovoltaic and light-emitting devices that utilize such singlet fission sensitization have not been as dramatic,[17−20,26−29] which may be related to slower charge transfer rates observed for triplet excitons.[30] Furthermore, recent studies of the separation of ^{1}(TT) intermediates and triplet transport in different polymorphs of pentacene derivatives revealed that triplet exciton transport underpins the dynamics that lead to triplet pair separation,[31−33] which depends on the strength of electronic coupling between neighboring molecules.[34] This was determined by demonstrating quantitative changes in both the rates of ^{1}(TT) separation and the triplet energy transfer rates (proportional to triplet diffusivity) in polycrystalline TIPS-Pn films.[31] These findings suggested that stronger electronic coupling would lead to improved triplet transport. However, recent investigations revealed that electronic coupling that is too strong can accelerate spin-allowed electronic relaxation processes similar to internal conversion[35] that can limit the ultimate yield of triplet exciton multiplication.[6]

This contrast between spectroscopic results and device studies highlights the need to elucidate the dynamics and structural factors that influence the rate and yield of ^{1}(TT) separation to form independent triplet excitons. This need is further emphasized by recent efforts to develop polymeric singlet fission sensitizers[2,3,36−41] because of their potential for facile thin film processing with a view toward incorporation into optoelectronic device structures. However, even the most highly ordered polymers such as high-density polyethylene contain significant fractions of an amorphous component.[42] Therefore, it is necessary to consider the influence that amorphous domains have on the dynamics of triplet pair formation, separation, and transport to understand how amorphous phases may affect the primary events leading to triplet pair separation and ultimately the overall yield of triplet exciton multiplication.

Polymeric singlet fission systems that inevitably contain amorphous regions have not demonstrated yields for long-lived triplet multiplication that are as high as crystalline systems for reasons that remain poorly understood.[2,3,36−41] Recent observations may provide some insight into this regard. Triplet diffusivity in amorphous domains of TIPS-Pn was found to be more than an order of magnitude smaller in comparison to their diffusivity in crystalline domains of the same material.[43] Other investigators reported exciton diffusion from disordered regions to "dimer" sites in nanocrystalline films using ultrafast measurements of singlet fission.[13,44] These and other papers[7,23,45−48] reported the sensitivity of the rate and yield of singlet fission to the intermolecular interactions and crystal structures of the materials. These intermolecular interactions may be yet more complex in the mixed amorphous/crystalline environment of polymeric systems being explored as next-generation singlet fission sensitizers.

In this work, we use ultrafast time-resolved infrared (TRIR) spectroscopy and electronic spectroscopy to study singlet fission reaction dynamics in purely amorphous and in polycrystalline TIPS-Pn films as a means to investigate the rates of ^{1}(TT) triplet pair separation vs transport in these environments. This work is motivated by prior studies, which showed that the vibrational modes of organic molecules such as TIPS-Pn are sensitive to the formation and separation of triplet excitons within the material.[11,49] TRIR spectroscopy is also used to directly probe the infrared electronic transitions of initially excited singlet states and ^{1}(TT) intermediates. Both measurements show that the spatial separation of ^{1}(TT) intermediates in amorphous TIPS-Pn films is surprisingly fast, occurring on the ∼6 ps time scale. This time scale is much faster than prior measurements of ^{1}(TT) triplet pair separation in amorphous nanoparticles of pentacene derivatives dispersed in solution[6] and is much closer to the 5 and 2.5 ps time scale observed in Form II brickwork and Form I brickwork phases of TIPS-Pn films that were reported previously.[31]

However, the rate of diffusion-controlled bimolecular triplet−triplet annihilation in the amorphous TIPS-Pn films studied here is dramatically slower in comparison to the crystalline films, causing triplet excited states to persist on time scales nearly an order magnitude longer than in the Form I brickwork polycrystalline film under the same excitation densities. This increase in lifetime is consistent with the order of magnitude reduction of the diffusivity of triplet excitons in amorphous phases of TIPS-Pn films.[43] Our findings suggest the presence of sparse triplet traps in the amorphous film environment that break the correlation of the rates of ^{1}(TT) separation and the triplet energy transfer that has been observed in crystalline systems.[31] This result further suggests that it may be possible to nanostructure amorphous singlet fission sensitizers such as polymers to enable efficient utilization of multiplied triplet excitons in photovoltaic and light-emitting applications despite their low diffusivity.

METHODS

As-cast TIPS-Pn films were prepared by first dissolving 20 mg of TIPS-Pn in 1 mL of dichloromethane. The resultant solution was then spin-cast onto 25 mm diameter, 1.5 mm thick CaF_2 substrates at 1000 rpm, producing amorphous TIPS-Pn films. To obtain polycrystalline films, as-cast TIPS-Pn films were solvent vapor annealed by using an apparatus previously described for 1 h.[43]

Visible absorption spectra of the TIPS-Pn samples were collected by using a commercially available instrument (Beckman, DU 520; Brea, CA). The spectra were background-subtracted by the CaF_2 substrate absorption. To measure the absorption spectra of TIPS-Pn solutions, a liquid film was formed by pressing a drop of TIPS-Pn solution between two CaF_2 optical flats.

Grazing-incidence X-ray diffraction (GIXRD) measurements were collected by using a PANalytical X'Pert Pro MPD diffractometer (PANalytical; Almelo, Netherlands). All samples were measured by using a 1° incident angle and Cu Kα radiation. All data were read and exported by using Jade 7.0 software.

Scanning electron microscopy (SEM) was completed with a Zeiss Merlin FE-SEM (Zeiss; Jena, Germany). Samples deposited and annealed on sapphire substrates were first

https://dx.doi.org/10.1021/acs.jpcc.0c07920
J. Phys. Chem. C 2020, 124, 23567−23578

coated with 30 Å of iridium to provide the conductive layer necessary for imaging. After loading, images were collected with acceleration voltages between 0.5 and 2.0 keV to limit electron penetration. For cross-sectional images, glass substrates coated with 40 nm gold were cleaved at room temperature across the center of the substrate.

Nanosecond transient absorption (TA) spectroscopy was performed by using an enVISion transient absorption spectrometer (Magnitude Instruments, State College, PA). The instrument utilized a home-built dye cavity pumped with a Continuum Surelite 30 Hz, 10 ns Nd:YAG laser (San Jose, CA). The output of the dye cavity (650 nm) was used as an excitation source. The continuous wave visible probe was dispersed through a monochromator before encountering the sample. The transmitted light was then collected by using lenses and detected with a photodiode.

Ultrafast TA spectroscopy in the visible spectral region was performed by using a home-built system previously described.[43] In brief, an optical parametric amplifier (OPA) (TOPAS, Light Conversion Ltd., Vilnius, Lithuania) was pumped by using 100 fs, 800 nm pulses produced by an amplified Ti:sapphire laser (Vitesse, Coherent, Santa Clara, CA/Integra-C, Quantronix, Santa Clara, CA). The output of the OPA was tuned to 650 nm to photoexcite the samples. The fundamental of the Ti:sapphire laser was focused onto a sapphire window (WG30530, Thorlabs; Newton, NJ) to create a white-light supercontinuum that was used as a probe source. The pump was mechanically delayed relative to the probe by using a motorized delay stage (IMS600CCHA, Newport; Irvine, CA). The probe beams were then detected by using a balanced silicon photodetector (PDB210A,Thorlabs; Newton, NJ).

FTIR absorption spectra were acquired by using a JASCO 6600 FTIR spectrometer equipped with a DTGS detector. All spectra were the average of 10 scans in the spectral range of 1200−3200 cm^{-1}. The spectra were background subtracted by the CaF_2 substrate absorption and baseline corrected by using a third-order polynomial. The resolution used for all FTIR experiments was 2 cm^{-1}.

Ultrafast TRIR TA spectra were collected by using a home-built system.[50] Two optical parametric amplifiers (OPAs) (TOPAS, Light Conversion Ltd., Vilnius, Lithuania) were pumped by using 100 fs, 800 nm pulses produced by an amplified Ti:sapphire laser (Vitesse, Coherent, Santa Clara, CA/Integra-C, Quantronix, Santa Clara, CA). The output of one OPA was tuned to 650 nm to photoexcite the samples while the other was tuned to produce mid-IR probe pulses between 2000 and 2200 cm^{-1}. Mid-IR probe pulses were dispersed through a monochromator (Triax, Horiba; Kyoto, Japan) and detected by using a 32 × 2 element MCT array detector (Infrared Associates/Infrared Systems Development; Stuart, FL). The resolution used for all TRIR experiments was ∼3.5 cm^{-1}.

It was found that the amorphous TIPS-Pn films could undergo slow thermal annealing if the ultrafast TRIR measurements were conducted on the same sample over too long a period of time. Fortunately, such thermal annealing could be observed by (1) changes of the absorption spectrum of the films evolving toward the Form II brickwork crystalline phase,[43] (2) the triplet−triplet annihilation kinetics accelerating due to enhanced triplet diffusivity in the crystalline environment,[31] (3) faster singlet fission dynamics on the picosecond time scale, and (4) the hot ground state absorption feature appearing in the transient vibrational spectra on the tens of picoseconds time scale.[11] We therefore conducted the ultrafast TRIR measurements of the amorphous films in the following manner to avoid this problem. Short data acquisition times of <20 min were used for each amorphous TIPS-Pn film sample so that the absorption spectrum and annihilation kinetics were unchanged over the course of each measurement. Fresh amorphous TIPS-Pn films were used for each measurement. That is, the amorphous TIPS-Pn film results presented in the article represent the average of several measurements on several different TIPS-Pn films. The averaging was done to improve the signal-to-noise ratio. The spectra and kinetics were similar across all the measurements averaged together. Finally, we confirmed that the amorphous films did not exhibit the indications (1), (2), or (3) above (see the Supporting Information), demonstrating that thermal annealing did not occur in the amorphous films during the course of the measurements reported here.

RESULTS AND DISCUSSION

Figure 1A depicts the visible absorption spectra of solvent annealed (amorphous) and as-cast (crystalline) TIPS-Pn films examined in this work that are compared with a spectrum of 20 mg/mL solution of TIPS-Pn molecules in dichloromethane that was used to spin-cast the films. The absorption spectrum of the solvent-annealed film exhibits broader vibronic features and is significantly red-shifted relative to the solution spectrum due to intermolecular electronic interactions in their crystalline packing arrangement. Crystalline polymorphs of TIPS-Pn have unique absorption spectra as reported previously.[43,51] Analysis of the absorption spectrum of the solvent annealed film presented in Figure 1A indicates that the TIPS-Pn molecules in the film adopt a highly ordered Form I brickwork packing arrangement, consistent with prior reports.[43] The absorption spectrum of the as-cast film resembles the solution spectrum but with broadened and red-shifted peaks, indicating that molecules in the as-cast film are weakly electronically coupled to each other in comparison to the solvent-annealed film. Figure 1B depicts SEM images of the as-cast (amorphous) and solvent-annealed (crystalline) TIPS-Pn films. The surface structure apparent in the crystalline film appears as TIPS-Pn molecules reorganize into crystalline domains during solvent annealing.

The solid-state order of the as-cast and solvent-annealed films examined here was investigated by using grazing-incidence X-ray diffraction (GIXRD) (Figure 1C). The diffraction pattern of the solvent-annealed film closely matches the diffraction pattern of TIPS-Pn films that adopt a Form 1 brickwork crystal structure.[31] Thus, solvent-annealed films, which are polycrystalline, are termed "crystalline" films here and in the following discussion. Conversely, the GIXRD pattern of the as-cast TIPS-Pn film of the same ∼100 nm thickness does not exhibit discernible features in the diffraction pattern, indicating a lack of crystallinity within the film. Because of this lack of long-range order, as-cast TIPS-Pn films are called "amorphous" films here and in the following.

Having characterized the structural properties of the amorphous and crystalline TIPS-Pn films, we examined the influence that intermolecular interactions and crystalline order have on the dynamics of singlet fission using TA spectroscopy. Figure 2A represents nanosecond TA spectra of the amorphous and crystalline TIPS-Pn films collected at 20 ns time delay between 450 and 600 nm following optical

https://dx.doi.org/10.1021/acs.jpcc.0c07920
J. Phys. Chem. C 2020, 124, 23567−23578

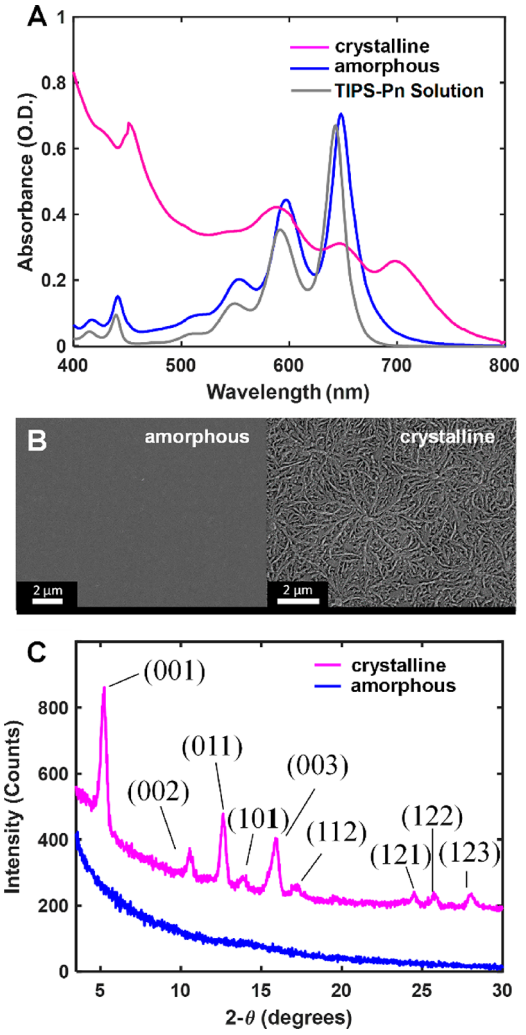

Figure 1. (A) Visible absorption spectra of as-cast (amorphous) and solvent-annealed (crystalline) TIPS-Pn films compared to the absorption spectrum of a TIPS-Pn solution. (B) SEM images of amorphous and crystalline TIPS-Pn films. Upon solvent annealing, crystalline structures protrude from the film surface, indicating reorganization of the molecules into polycrystalline domains. (C) Grazing-incidence X-ray diffraction patterns measured for solvent-annealed and as-cast TIPS-Pn films. The diffraction patterns are offset for clarity.

excitation at 650 nm (50 μJ/cm^2), which we use to establish assignments of transitions in the visible spectral range. The absorption features appearing in Figure 2A were previously assigned to the $T_1 \rightarrow T_n$ transition of the correlated triplet pair intermediates (^{1}(TT) and ^{1}(T...T)) and of triplet excitons (T_1) that have overlapping spectral features.[52,53] We use this assignment and will refer to the $T_1 \rightarrow T_n$ transitions in Figure 2A as the triplet absorption spectra here and in the following. The triplet absorption spectrum of the crystalline film exhibits a red-shift in comparison to the amorphous film due to increased intermolecular interactions between TIPS-Pn molecules in their crystalline packing arrangements. This observation is consistent with an earlier report that the triplet absorption spectrum of TIPS-Pn depends on the strength of intermolecular interactions in the solid state.[35]

Figure 2B compares the growth kinetics of the triplet absorption spectra measured in the amorphous and crystalline TIPS-Pn films between 0 and 50 ps time delays following

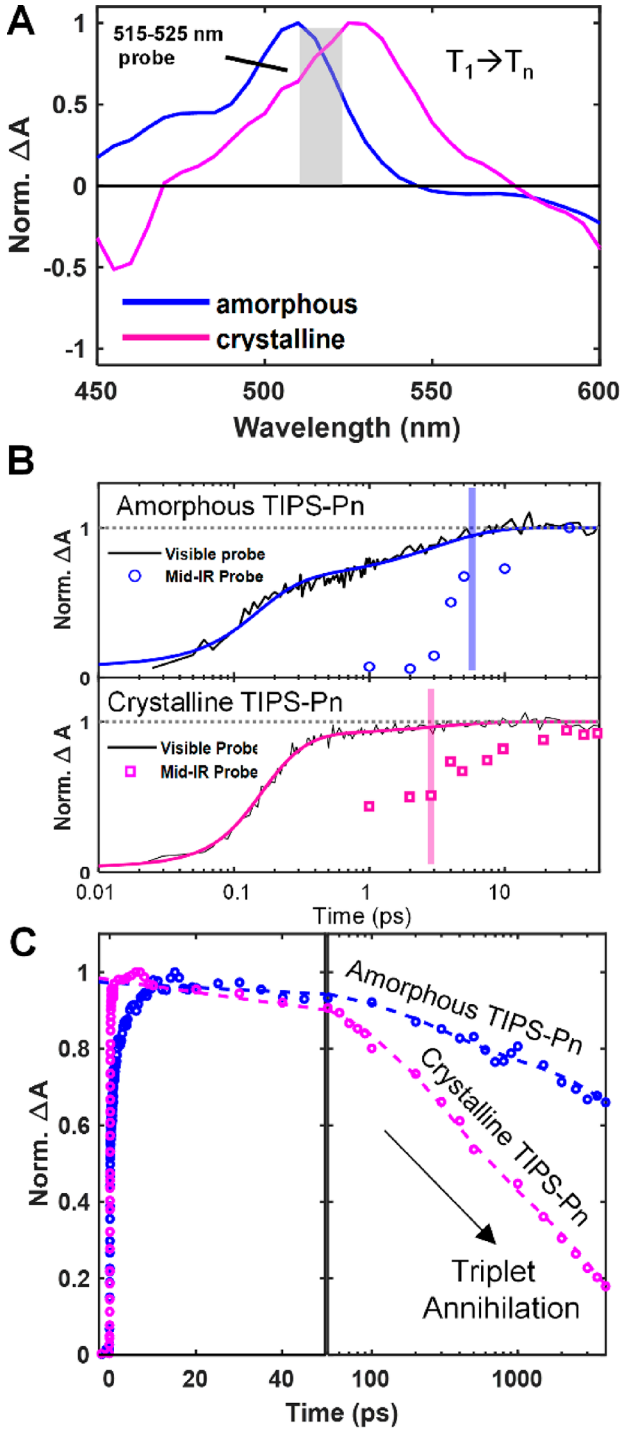

Figure 2. (A) Transient absorption spectra of triplet excitons in the visible spectral region measured in amorphous and crystalline TIPS-pentacene films collected at a 20 ns time delay. (B) Transient absorption kinetics obtained by integrating the spectral region between 515 and 525 nm following optical excitation at 650 nm. The kinetics highlight the growth of the triplet absorption feature in amorphous and crystalline TIPS-Pn films between a 0 and 50 ps time delay. Note the logarithmic axis. The solid lines represent biexponential fits to the data. The symbols represent the growth of the triplet population dynamics obtained from analysis of TIPS-Pn film's alkyne stretch mode in the mid-IR. (C) Comparison of the transient absorption kinetics obtained by integrating the spectral region between 515 and 525 nm plotted on a linear time axis before 50 ps and a logarithmic time axis afterward to emphasize differences in the triplet−triplet annihilation kinetics.

https://dx.doi.org/10.1021/acs.jpcc.0c07920
J. Phys. Chem. C 2020, 124, 23567−23578

optical excitation at 650 nm (150 μJ/cm^2). The kinetics result from integration of the TA signal between 515 and 525 nm, which is indicated by the gray shaded region in Figure 2A. The time origin of the kinetics traces have been shifted by 100 fs to capture the pulse-limited rise component on the logarithmic time axis. We note that the growth kinetics displayed in Figure 2B were collected on a different time scale than the spectra appearing in Figure 2A. However, prior TA measurements have assigned the sub-50 ps growth of the kinetics appearing in Figure 2B to the separation of singlet fission intermediates into triplet excitons.[4,48]

We quantified the growth of the TA signal appearing in Figure 2B using the sum of two exponential growth functions given by

$$F(t) = f(t) * g(t)$$

$$f(t) = N_1[a_1(1 - e^{-t/\tau_1}) + (1 - a_2)(1 - e^{-t/\tau_2})] \quad (2)$$

$$g(t) = N_2 \exp\left[-\frac{1}{4}\left(\frac{t}{\gamma/2\ln(2)}\right)^2\right] \quad (3)$$

where $g(t)$ is an area-normalized Gaussian function used to represent the instrument response function of our ultrafast TA instruments, t is time, N_1 and N_2 are normalization constants, a_1 and a_2 are scaling factors, τ_1 and τ_2 are the lifetimes of the exponential functions, and γ is the full width at half-maximum of the Gaussian function (~100 fs). Table 1 summarizes the results of the fits.

Table 1. List of Best-Fit Parameters Obtained by Fitting the Triplet Growth Kinetics Appearing in Figure 2B with Eqs 2 and 3

sample	a_1	T_1 (ps)	τ_2 (ps)	$\langle\tau\rangle$ (ps)
crystalline	0.90 ± 0.02	0.11 ± 0.01	3.0 ± 0.2	0.40 ± 0.3
amorphous	0.69 ± 0.01	0.10 ± 0.02	3.2 ± 0.3	1.06 ± 0.3

The data reveal that the triplet absorption feature exhibits a fast rise component on the subpicosecond time scale that has been assigned to the primary singlet fission reaction to form ^{1}(TT) intermediates.[4,44] As noted earlier, the slower rise component that occurs on the sub-10 ps time scale in both the amorphous and crystalline TIPS-Pn films is believed to indicate the spatial separation of ^{1}(TT) states in pentacene derivatives.[4,48] The separation of triplets from ^{1}(TT) intermediates increases their absorption cross section, leading to greater extinction coefficients of ^{1}(T...T) states than for proximal ^{1}(TT) intermediates.[4] We note that the slow rise component in the amorphous film may also include a contribution from dispersive excitation energy transport due to energetic disorder in the amorphous environment. Nonetheless, the data and fit results (Table 1) indicate that the combination of dispersive energy transport and triplet pair separation in the amorphous film occurs on the sub-10 ps time scale, suggesting that ^{1}(TT) intermediates separate on time scales similar to the crystalline film.

Figure 2C depicts an overlay of the same TA kinetics traces but plotted with a linear time axis between 0 and 50 ps and a logarithmic axis for longer time delays. The representation emphasizes the differences in the decay kinetics of the TA signals measured in the amorphous and crystalline films. Previous excitation energy density dependent measurements in crystalline TIPS-Pn films demonstrate that the decay of the TA signal of triplet excitons on later time scales in the crystalline film is due to bimolecular triplet−triplet annihilation.[18,20] We therefore assign the decay kinetics represented in Figure 2C to be dominated by triplet−triplet annihilation in both amorphous and crystalline TIPS-Pn films. The dashed lines through the TA data in Figure 2C represent biexponential fit functions that were used to quantify the time scale for triplet−triplet annihilation in the measurements. It is noteworthy that triplet−triplet annihilation occurs on a time scale nearly an order of magnitude longer in the amorphous vs the crystalline film (Table 2), which is consistent with the order of magnitude lower diffusivity of triplet excitons in amorphous domains of TIPS-Pn.[43]

The TA data in Figure 2 suggest that triplet pair separation from ^{1}(TT) intermediates in the amorphous and crystalline TIPS-Pn films occurs on similar time scales despite the significantly different intermolecular electronic interactions in these films (indicated by differences in their electronic absorption spectra, Figure 1A). The time scale of the slower growth component of the TA kinetics measured in the amorphous film (assigned to triplet pair separation) is actually very similar to the time scale for triplet pair separation from ^{1}(TT) intermediates reported in the Form II brickwork phase of TIPS-Pn[31] even though the amorphous film lacks long-range order (Figure 1C). Note the precautions that were taken to ensure the amorphous films did not undergo thermal annealing during the measurements (see the Methods section). Because these findings were surprising to us, we desired an alternate method to investigate the dynamics of triplet pair separation from ^{1}(TT) intermediates to validate these observations. Therefore, we used ultrafast TRIR spectroscopy to characterize the time scale at which ^{1}(TT) intermediates separate in the TIPS-Pn films examined here.

TRIR spectroscopy has emerged as a technique capable of examining the influence that molecular structure has on electronic processes in optoelectronic materials due to the sensitivity of molecular vibrations to their local environment.[54] For example, nitrile (CN) vibrational modes of molecules were used to probe electron transfer reactions between small molecule donors and acceptors following optical excitation.[55] Likewise, TRIR spectroscopy was used to study exciton localization in perylene diimide films,[56] ligand−nanocrystal interactions on the surfaces of colloidal quantum dots,[57] and excited-state vibrational dynamics in halide perovskites.[58,59]

Table 2. List of Best-Fit Parameters from Fitting the Longer Time Scale Components of the TA Decay Traces Appearing in Figure 2C[a]

sample	a_1	τ_1 (ps)	τ_2 (ps)	τ_{ave} (ps)
crystalline	0.43 ± 0.06	240 ± 20	(3.4 ± 0.1) × 10^3	(2.1 ± 0.4) × 10^3
amorphous	0.18 ± 0.02	150 ± 20	(1.7 ± 0.2) × 10^4	(1.4 ± 0.3) × 10^4

[a]The decay of the TA signal is due to triplet−triplet annihilation.

https://dx.doi.org/10.1021/acs.jpcc.0c07920
J. Phys. Chem. C 2020, 124, 23567−23578

Recently, TRIR spectroscopy was used to investigate the dynamics of singlet fission in polycrystalline TIPS-Pn films.[10] In that work, the alkyne stretch modes of the TIPS-Pn molecule's triisopropylsilylethynyl (TIPS) side groups were used to probe the dynamics of electronic states involved in the singlet fission reaction. By monitoring the native vibrational modes of the TIPS-Pn molecules, the authors determined the time scale on which ^{1}(TT) intermediates separated in crystalline TIPS-Pn films. Additionally, broad electronic transitions of ^{1}(TT) intermediates were examined in the mid-IR, providing an independent probe of their formation and separation. We adopted the same approach to investigate the separation of ^{1}(TT) intermediates in the amorphous vs the crystalline TIPS-Pn films examined here.

Figure 3A displays the ground-state FTIR spectra of amorphous and crystalline TIPS-Pn films examined in this work. Figure 3B highlights the alkyne stretch modes of the TIPS-Pn films for comparison to the vibrational features that appear in the ultrafast TRIR spectra described below. The chemical structure of the triisopropylsilylethynyl (TIPS) side groups appears in the figure for reference. Because the alkyne stretch mode appears in an uncongested region of the mid-IR spectrum and is coupled to the conjugated framework of the molecules,[49] it serves as a probe suited to track the dynamics of the transient electronic states of the material.[11]

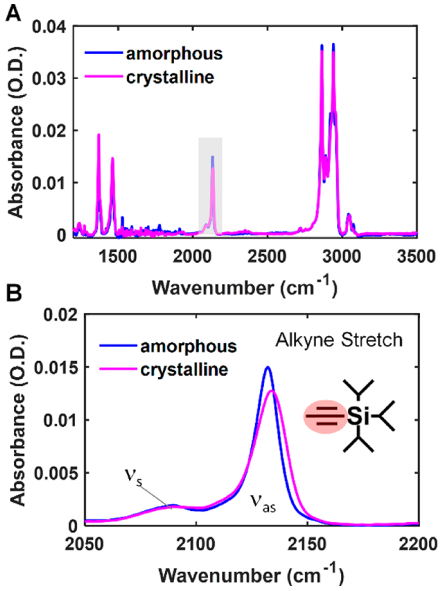

Figure 3. (A) FTIR spectra of amorphous and crystalline TIPS-Pn films. The gray shaded box highlights the alkyne stretch modes of the films. (B) FTIR spectra of amorphous and crystalline TIPS-Pn films collected in the alkyne stretch region. The chemical structure of the TIPS-Pn molecule's triisopropylsilylethynyl (TIPS) side groups is included for reference.

Figure 4A displays ultrafast TRIR spectra of crystalline and amorphous TIPS-Pn films measured in the alkyne stretch region at early (1−10 ps) and late (100−1000 ps) time delays following optical excitation at 650 nm (150 μJ/cm^2). The TRIR spectra presented in Figure 4A exhibit a broad electronic absorption offset in the mid-IR that arises from the photoexcitation of singlet excitons and ^{1}(TT) intermediates formed in the primary steps of the singlet fission reaction (dotted lines, Figure 4A).[5] The origin of the broad mid-IR absorption has been assigned to a transition from singlet

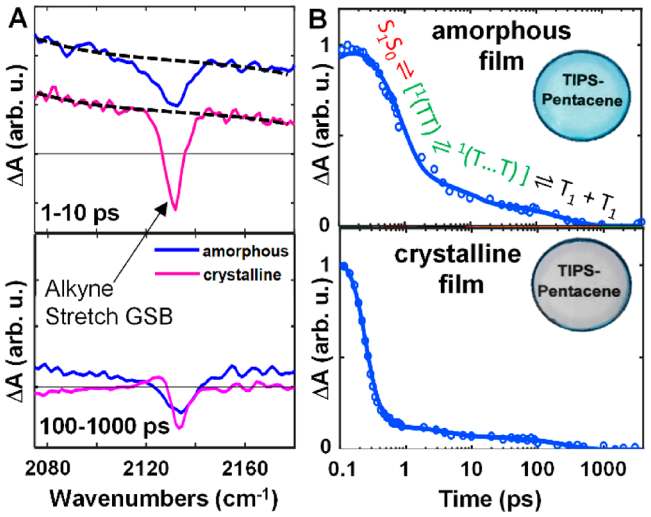

Figure 4. (A) Ultrafast TRIR spectra of amorphous and crystalline TIPS-pentacene films obtained by averaging several spectra at early (1−10 ps) and late (100−1000 ps) time delays following 650 nm excitation (~150 μJ/cm^2). The dashed lines highlight the broad absorption offset superimposed on the alkyne stretch vibrational feature. The prominent ground state bleach (GSB) of the films is indicated in the figure. (B) Decay kinetics of the broad absorption offset. The broad absorption offset decays due to the formation of ^{1}(TT) and ^{1}(T...T) intermediates and then the subsequent separation of these intermediates into separated triplet excitons on longer time scales. The insets show photographic images of the amorphous and crystalline TIPS-Pn films.

electronic states to higher-lying multiexciton (ME) states. Superimposed on this broad mid-IR absorption offset are narrow vibrational features of the alkyne stretch modes of TIPS-Pn molecules involved in the singlet fission reaction.

Figure 4B represents the decay traces of the broad mid-IR absorption offsets measured in both the amorphous and crystalline TIPS-Pn films. Note the logarithmic time scale. The kinetic traces were obtained by integrating the spectral region between 2080 and 2120 cm^{-1}. Prior TRIR measurements of crystalline TIPS-Pn films demonstrated that the subpicosecond decay of the broad mid-IR absorption offset arises from the formation of ^{1}(TT) intermediates following the primary steps in singlet fission.[5] The slower decay of the broad mid-IR absorption was assigned to the separation of triplet pairs from the ^{1}(TT) intermediates, which occurred on a range of time scales due to the ability to re-form triplet pair states by triplet fusion.[5,15]

The data in Figure 4B suggest that the sequence of steps in the singlet fission reaction (eq 1) occurs more slowly in the amorphous TIPS-Pn film, but not dramatically so, in comparison to the crystalline film. For example, the initial decay of the broad mid-IR absorption in the amorphous film on the ~0.5 ps time scale suggests that the dynamics to form the ^{1}(TT) intermediates are somewhat slower than in the crystalline film. Several studies have suggested that triplet transfer mediates triplet pair separation in crystalline TIPS-Pn films[31−33] and that this process depends on the strength of intermolecular coupling between molecules.[34] Thus, the slower triplet pair separation rate in amorphous TIPS-Pn films may be due to a reduction in the average intermolecular coupling between neighboring TIPS-Pn molecules.

The subsequent decay of the broad electronic absorption in Figure 4B results from complex kinetic processes that occur on

https://dx.doi.org/10.1021/acs.jpcc.0c07920
J. Phys. Chem. C 2020, 124, 23567−23578

time scales too similar in the amorphous and crystalline films to distinguish them by visual inspection of the data. Therefore, we analyzed the decay kinetics using a kinetic model that was reported previously.[5,35] In particular, we modeled the decay of the broad absorption offset using a system of coupled rate equations that describe the singlet fission reaction given by

$$\frac{d[S_1S_0]}{dt} = -k_1[S_1S_0] \quad (4)$$

$$\frac{d[^1(TT)]}{dt} = +k_1[S_1S_0] - k_2[^1(TT)] + k_{TF}[^1(T...T)] \quad (5)$$

$$\frac{d[^1(T...T)]}{dt} = +k_2[^1(TT)] - k_{TF}[^1(T...T)] - \frac{1}{2}k_3[^1(T...T)] \quad (6)$$

$$\frac{d[T_1]}{dt} = +2k_3[^1(T...T)] - \frac{1}{2}k_4[T_1]^2 \quad (7)$$

where k_i are rate constants and t is time. In this model, $^1(TT)$ and $^1(T...T)$ represent correlated triplet pair intermediates that are proximal or that have separated as defined in eq 1. The rate constant k_1 is the rate of singlet fission for form $^1(TT)$ intermediates, k_2 is the rate of triplet pair separation, k_{TF} is the rate of fusion of triplet pairs to re-form the $^1(TT)$ intermediate, k_3 is the rate of complete separation of triplet pairs to form states with negligible probability of fusing again, and k_4 is the rate of triplet−triplet annihilation which is related to the diffusivity of the triplets within the material.[20,60,61]

The coupled rate equations above were solved numerically using the conditions: $[S_1S_0]_{t=0} = 1$, $[^1(TT)]_{t=0} = 0$, $[^1(T...T)]_{t=0} = 0$, and $[T_1]_{t=0} = 0$. Normalized kinetics traces measured from the broad mid-IR absorptions in the amorphous and crystalline films are represented in Figure 5 which are overlaid with the best fit functions obtained from a linear combination of the kinetics of the appropriate absorbing species described by

$$\frac{\Delta A_{\text{mid-IR}}(t)}{\Delta A^{\max}_{\text{mid-IR}}} = a_1[S_1S_0](t) + a_2[^1(TT)](t) + a_3[^1(T...T)](t) \quad (8)$$

Here, the a_i are fit parameters related to the mid-IR absorption cross sections of the transient electronic states. We used a nonlinear least-squares fitting routine to fit the broad electronic absorption kinetics. The smooth curves overlaid on the data (circles) in Figure 5B show that the kinetic model provides an accurate description of kinetics over their full time and amplitude variation. Figure 5C highlights the lower amplitude, longer time scale portion of the kinetics to demonstrate the fidelity of the fits. The time evolution of the populations of transient electronic states represented by the kinetic model appear above the kinetics in Figure 5A for reference. The best fit parameters and corresponding uncertainty limits from the analysis are represented in Table 3. The rates of triplet pair separation, k_2, for the amorphous and crystalline films obtained from the analysis are highlighted in Figure 5C for emphasis.

The population dynamics obtained from modeling the broad mid-IR absorption kinetics in Figure 5 reveal that the initial spatial separation of $^1(TT)$ intermediates occurs on the 6.2 ± 0.2 and 3.1 ± 0.5 ps time scales in amorphous and crystalline TIPS-Pn films, respectively. These time constants are quantitatively consistent with the slower rise components of the triplet absorption kinetics measured in the visible region

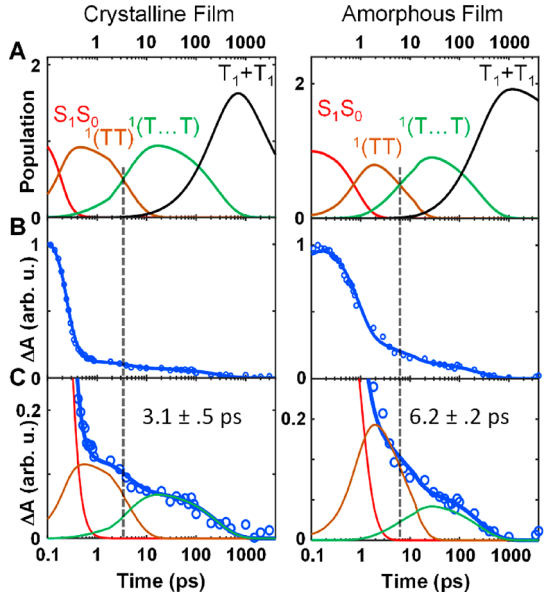

Figure 5. (A) Population dynamics of the singlet fission reaction in crystalline and amorphous TIPS-Pn films obtained by fitting the decay kinetics of the broad mid-IR absorption feature appearing in Figure 4B. (B) Best fits to the mid-IR decay kinetics. (C) Expanded region of the mid-IR decay trace. The best fit (blue solid line) and the fit components for each population are shown in the figure. The dashed black lines indicate the approximate time at which correlated triplet pairs spatially separation in each film.

represented in Figure 2B and summarized in Table 1. Importantly, the data indicate that in both films the $^1(TT)$ and $^1(T...T)$ intermediates persist for hundreds of picoseconds,[5] suggesting that the triplet pair separation and fusion processes that ultimately lead to independent triplets occur on similar time scales in both amorphous and crystalline films. Independent triplet excitons do not appear to form on the picosecond time scale within either material.

We note that we do not have distinct spectroscopic features for $^1(T...T)$ states that differ from T_1 states even though we represent these populations in the kinetic model. This would require a magnetic field, which we did not use in the measurements reported here. Our measurements do provide distinct spectroscopic features of $^1(S_1S_0)$, $^1(TT)$, and spatially separated $^1(T\cdots T)$ states. We rely on kinetic modeling of the $^1(TT)$, $^1(T\cdots T)$, and $2T_1$ species that we derive from recent literature reports and our prior work[5,15] to describe what the kinetics of $^1(T\cdots T)$ vs $2T_1$ states may have been to properly describe the mid-IR TA spectra and kinetics in Figure 5. From this modeling, we obtain the population kinetics of $^1(T\cdots T)$ vs $2T_1$ states.

We sought to gain additional information about the dynamics of triplet pair separation and triplet transport that might provide insight about the limited yields of triplet multiplication observed in amorphous and polymeric singlet fission sensitizers. Therefore, we utilized the sensitivity of vibrational modes to the presence of excited electronic states to track the evolution of triplet excited states during the singlet fission process.[11,49] Figure 6 depicts baseline-corrected ultrafast TRIR spectra of the amorphous and crystalline TIPS-Pn films from which we analyzed the vibrational features. The transient vibrational spectra were obtained by subtracting the best fit of the broad mid-IR absorption offsets appearing in Figure 4A from the data for each time point measured in the experiment.

https://dx.doi.org/10.1021/acs.jpcc.0c07920
J. Phys. Chem. C 2020, 124, 23567−23578

Table 3. List of Best-Fit Parameters Obtained by Fitting the Decay Traces Appearing in Figure 5

sample	a_1	a_2	a_3	k_1 (ps^{-1})	k_2 (ps^{-1})	k_{TF} (ps^{-1})	k_3 (ps^{-1})	k_4 (ps^{-1})
crystalline	0.98	0.13	0.07	12.0	0.30	0.01	4.1×10^{-3}	5×10^{-4}
amorphous	0.93	0.28	0.12	2.0	0.16	0.01	3.5×10^{-3}	7×10^{-5}

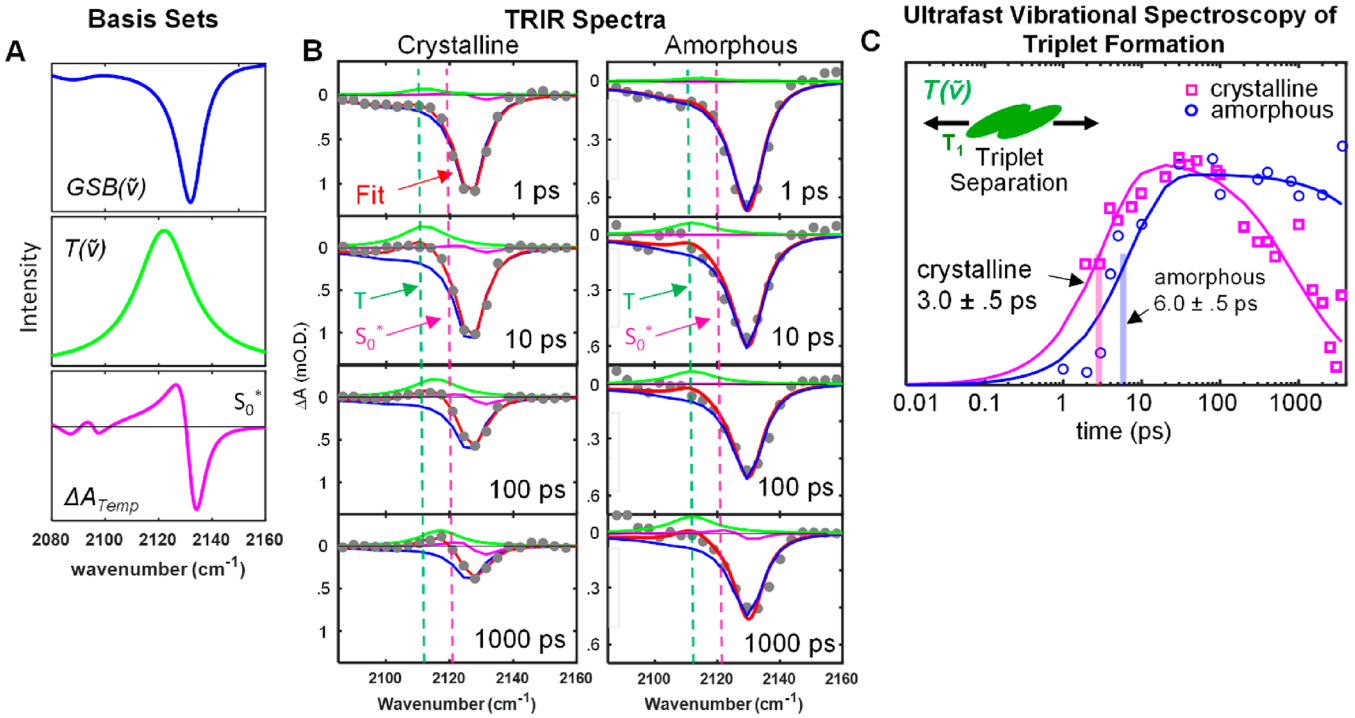

Figure 6. (A) Basis spectra used to fit the ultrafast vibrational transient absorption spectra of crystalline and amorphous TIPS-pentacene films. The GSB and S_0* spectra were measured by using FTIR spectroscopy. (B) Baseline-corrected ultrafast time-resolved infrared (TRIR) spectra of crystalline and amorphous TIPS-pentacene films measured in the alkyne stretch region at 1, 10, 100, and 1000 ps following optical excitation at 650 nm (150 $\mu J/cm^2$). The spectra are overlaid with the best fit spectra (red lines). The basis spectra of the GSB, triplet (T), and hot ground state S_0* are overlaid on the data to highlight the characteristic time evolution of the transient populations. (C) Comparison of separated triplet formation and decay kinetics in the amorphous and crystalline TIPS-Pn films obtained from analysis of the $T(\tilde{\nu})$ vibrational feature. Triplet pair separation occurs on similar time scales in both films, but triplet−triplet annihilation occurs much more slowly in the amorphous film under comparable conditions.

The TRIR spectra presented in Figure 6 were modeled by using a method previously developed to monitor the population of triplet excitons during the singlet fission reaction.[10] A complete description of this method is given in the Supporting Information. In brief, the TRIR spectra were modeled using the sum of three basis functions given by

$$F(\tilde{\nu}) = n_1 \mathrm{GSB}(\tilde{\nu}) + n_2 T(\tilde{\nu}) + n_3 \Delta A_{\mathrm{Temp}}(\tilde{\nu}) \quad (9)$$

where $\tilde{\nu}$ is frequency in units of wavenumbers, $\mathrm{GSB}(\tilde{\nu})$ is the inverted FTIR spectrum for each sample, $T(\tilde{\nu})$ is a skewed Lorentzian function, and ΔA_{Temp} is the temperature difference spectrum of the alkyne stretch of the hot ground state obtained from temperature-dependent FTIR measurements (see the Supporting Information). These basis functions are shown in Figure 6A for reference. The best fits obtained from fitting the TRIR spectra with eq 9 (red lines) are overlaid onto the data (circles) in Figure 6B. For comparison, the corresponding basis spectra scaled according to their best fit amplitudes also are shown in each panel. Note that the shapes of the $\mathrm{GSB}(\tilde{\nu})$ and ΔA_{Temp} spectra were determined experimentally. Only the shape of the $T(\tilde{\nu})$ is a skewed Lorentzian function that was adjusted during the fitting procedure. This approach constrained the fitting procedure and permitted us to analyze the population dynamics from the evolution of TRIR spectra with high fidelity.

On early time scales (~1 ps), the TRIR spectra of both the amorphous and crystalline TIPS-Pn films (top of Figure 6B) match the inverted FTIR spectra $\mathrm{GSB}(\tilde{\nu})$ of the samples (Figure 3B and reproduced in Figure 6A). However, by 10 ps the transient vibrational features of both films begin to deviate from the inverted FTIR spectra due to the formation of a new electronic state that has a distinct alkyne stretch at lower frequency relative to the ground state bleach feature. For example, the best fit curves overlaid on the 10 ps spectra of both films are well described by the sum of the inverted FTIR spectrum (blue curves) and the positive peak of this new electronic state $T(\tilde{\nu})$ (green curves). Prior TRIR measurements of TIPS-Pn assigned the $T(\tilde{\nu})$ vibrational feature to the alkyne stretch mode of spatially separated triplet pairs ^{1}(T...T) and triplet excitons (T_1).[11,49] We note that the underlying reason we observe a distinct alkyne stretch frequency for spatially separated and independent triplet excitons but not for singlet excitons or proximal triplet pairs remains an interesting area of investigation.[49] We speculate that the change in frequency is related to a change in electron density near the alkyne groups caused by variation of the spatial component of

https://dx.doi.org/10.1021/acs.jpcc.0c07920
J. Phys. Chem. C 2020, 124, 23567−23578

the electronic states that must accompany the spin transition from singlet to triplet states.

On longer time scales, a second absorption feature centered at ~2124 cm^{-1} appears in the 100 and 1000 ps TRIR spectra of the crystalline film presented in Figure 6B (magenta curves). Comparison of this vibrational feature with the temperature difference FTIR spectra measured in the TIPS-Pn films ΔA_{Temp} (ΔT = 345 K − 295 K) reveals that it arises from heat deposited into the film as a result of electronic and vibrational relaxation processes. This feature is most clearly observed in the crystalline TIPS-Pn film, which undergoes faster triplet−triplet annihilation (Figure 2C). Interestingly, the ΔA_{Temp} feature does not contribute significantly to the TRIR spectra of the amorphous pentacene film in comparison to the crystalline film. This is consistent with the reduction of the rate of triplet−triplet annihilation that gives rise to the longer-lived triplet absorption kinetics trace in the amorphous film. We note that the absence of the ΔA_{Temp} feature in the amorphous film serves as an internal indicator that the film did not thermally anneal to form a crystalline phase during the course of the experiments.

Fitting the TRIR spectra at each time point by using eq 9 permitted us to analyze the population dynamics of separated triplet states in the amorphous and crystalline TIPS-Pn films through their $T(\tilde{\nu})$ vibrational features. Figure 6C displays the triplet population kinetics for each film obtained by plotting the area of the $T(\tilde{\nu})$ vibrational feature in each film as a function of time. Similarly, the dynamics of the hot ground state population S_0* are obtained from the ΔA_{Temp} feature and shown in the Supporting Information. The growth of the triplet population in each film was quantified by using a kinetic model that takes into account the separation of ^{1}(TT) intermediates to spatially separated triplets (see the Supporting Information) and their subsequent decay, which is dominated by triplet−triplet annihilation.[18,20] From the exponential fits, we determined that triplet pair separation from ^{1}(TT) intermediates occurred on the 6 ± 0.5 and 3 ± 0.5 ps time scales in amorphous and crystalline TIPS-Pn films, respectively. These time scales are in quantitative agreement with the results obtained from analysis of the broad mid-IR absorption kinetics traces appearing in Figure 5. Note that the open symbols appearing in Figure 2B for the amorphous and crystalline films represent the time dependent rise of the $T(\tilde{\nu})$ vibrational features obtained from the analysis of the transient vibrational spectra described here. The vertical lines marking the time constants of the rise of the $T(\tilde{\nu})$ vibrational features match the slow rise components observed in the triplet absorption kinetics traces, consistent with prior assignments that both metrics indicate the time scale for separation of ^{1}(TT) intermediates. Consequently, we conclude that triplet pair separation from ^{1}(TT) intermediates occurs on similar time scales in the amorphous film as is observed in crystalline TIPS-Pn films despite the lack of long-range order in the amorphous environment.

We note that prior reports of triplet pair separation in amorphous nanoparticles suggested that the process occurs on longer time scales.[6] We speculate that amorphous nanoparticles formed by rapid injection of concentrated TIPS-Pn solutions into water in that work[6] may differ in structure from the amorphous TIPS-Pn films spin-cast from dichloromethane solutions examined here. The dry-down time for the spin-cast film is longer than the abrupt precipitation of nanoparticles in water. It is likely that TIPS-Pn molecules in the amorphous nanoparticles had weaker average intermolecular interactions and slower triplet pair separation dynamics in comparison to amorphous TIPS-Pn films examined here.

Finally, we consider the implications of the differences in triplet decay kinetics appearing in Figures 2C and 6C. Both measures of the triplet population dynamics reveal that triplets decay much more slowly in the amorphous film under the same excitation intensity conditions. It is understood that the density of triplet excitons may be lower in the amorphous TIPS-Pn film because the yield of triplet exciton formation has been estimated to be ~75% of the yield observed in the crystalline film.[43] This and the similarity in time scale of the triplet separation dynamics k_2 and k_3 obtained from kinetic modeling of the amorphous and crystalline films in Figure 5C and Table 3 suggest that triplets have comparable potential to separate in both films. Therefore, we do not believe the nearly order of magnitude variation in triplet decay time can be explained by differences in triplet densities in the amorphous vs the crystalline TIPS-Pn films.

The observation of similar time scales for ^{1}(TT) separation but markedly different time scales for triplet−triplet annihilation in the amorphous vs the crystalline TIPS-Pn films is intriguing. We recall that the process by which ^{1}(TT) intermediates separate in TIPS-Pn and the diffusion of triplet excitons both involve triplet energy transfer.[31−33] For example, a recent report demonstrated that the rate of ^{1}(TT) separation k_2 (eq 6) and the bimolecular constant for triplet−triplet annihilation k_4 (eq 7) varied in direct proportion to each other comparing different polymorphs of TIPS-Pn.[31] If the amorphous film behaved similarly, we would anticipate only a factor of 2 change in the time scale for triplet−triplet annihilation. The amorphous film by contrast exhibits a nearly order of magnitude increase in the time scale for triplet−triplet annihilation (Table 2 and Figure 6C), indicating that triplets diffuse more slowly in the amorphous environment. This result is consistent with previous reports that demonstrated a marked reduction in the bimolecular rate constant k_{bi} for triplet−triplet annihilation in amorphous TIPS-Pn films.[43]

The similarity in time scale of the triplet separation dynamics of the amorphous and crystalline films combined with the markedly lower triplet diffusivity and slower annihilation kinetics suggests that states exist in the amorphous TIPS-Pn film that inhibit triplet energy transfer. For example, prior results demonstrated that triplet excitons in amorphous films have shorter exciton diffusion lengths (~20 nm) than they have in Form I brickwork crystalline films (~80 nm).[43] Because the triplet pair separation and fusion dynamics on the 100 ps time scale[5] are similar in both amorphous and crystalline films (Figure 5C), we conclude that these states are relatively sparse. We will refer to these states that impede triplet transport as triplet traps, although the nature of such triplet trap states remains to be determined. We note that time-resolved fluorescence measurements in amorphous TIPS-Pn films revealed the presence of states that trapped singlet excitons, which enabled fluorescence to be detected from TIPS-Pn molecules in the amorphous film environment.[5]

We speculate that the structural disorder that gives rise to such states may also lead to the trapping of triplet excitons. For example, the amorphous TIPS-Pn films examined here may contain a distribution of structures and intermolecular coupling strengths. Thus, while the average intermolecular coupling in amorphous TIPS-Pn films is low (based on its absorption spectrum, Figure 1A), there may be clusters of molecules that

https://dx.doi.org/10.1021/acs.jpcc.0c07920
J. Phys. Chem. C 2020, 124, 23567−23578

experience stronger coupling, affecting singlet fission and triplet pair separation rates. Conversely, there may be clusters of molecules that experience such low intermolecular coupling as to appear isolated in the film. Molecules in such locations may be responsible for the observation of fluorescence from singlet states in the amorphous film[5] and also may serve as triplet traps due to the low diffusivity that triplets would experience once they encountered such isolated states.[43] In this latter case, triplet traps would function in this role not because of energetic disorder but because of kinetic trapping due to low electronic coupling with their neighboring molecules. We believe that future work which investigates the structural characteristics of the TIPS-Pn films that lead to triplet traps will provide important information regarding the formation of such states in amorphous materials.

The presence of sparse triplet traps in amorphous TIPS-Pn films suggests a plausible explanation for the modest triplet multiplication yields that have been observed in polymeric singlet fission sensitizers.[2,3,36−41] For example, recent work has suggested that excimer formation in amorphous TIPS-Pn nanoparticles may cause ^{1}(TT) intermediates to return to their ground electronic state before separation.[6] We speculate that, like amorphous TIPS-Pn films, polymeric singlet fission sensitizers may contain triplet traps that reduce the diffusivity of triplets formed from singlet fission and may accelerate excited state relaxation processes that compete with the separation of multiplied triplet excitons following singlet fission.

The observation of rapid triplet pair separation in amorphous TIPS-Pn films that is comparable to polycrystalline systems suggests that it may be possible to utilize amorphous or mixed phase singlet fission sensitizer systems and polymers in practical applications. The presence of sparse triplet trap states in amorphous films suggests two approaches going forward. One approach would seek to identify the structural origins of triplet traps and find molecular structures that self-assemble in patterns that avoid them. Another approach would nanostructure amorphous or polymeric singlet fission sensitizers so that triplet excitons do not need to diffuse far to be harvested. This approach may have the advantage of allowing triplet traps to accelerate the decorrelation of triplets from their spatial and spin pair states following singlet fission. This could enhance the overall yield for harvesting multiplied triplet excitons by avoiding relaxation processes that can occur before such pair states separate.

CONCLUSION

In this work, the separation of triplet pair intermediates in amorphous and crystalline TIPS-Pn films was monitored by using time-resolved infrared and electronic transient absorption spectroscopy. In both amorphous and crystalline TIPS-Pn films, triplet pair intermediates were shown to spatially separate on the sub-10 ps time scale, despite TIPS-Pn molecules in the amorphous film lacking long-range order. The irreversible separation of these intermediates occurred on the hundreds of picoseconds time scale and likely involved multiple triplet separation and fusion events. The similarity of the singlet fission reaction dynamics in both amorphous and crystalline TIPS-Pn films suggests that materials with low crystalline order, such as polymers, can be utilized in singlet-fission sensitized photovoltaic or light-emitting devices. However, measurements of diffusion-controlled triplet−triplet annihilation revealed that triplet transport in amorphous films occurred much more slowly in comparison to crystalline films. The data suggest the presence of sparse states in the amorphous environment that inhibit long-range triplet transport. The presence of such states, which we call triplet traps, may provide insight about why low triplet multiplication yields have thus far been observed in polymeric singlet fission sensitizers. The fast rates of triplet pair separation in both crystalline and amorphous environments of TIPS-Pn observed here suggest that it may be possible to nanostructure amorphous or polymeric singlet fission sensitizers to efficiently harvest multiplied triplets despite their low diffusivity in the amorphous environment.

ASSOCIATED CONTENT

Supporting Information

The Supporting Information is available free of charge at https://pubs.acs.org/doi/10.1021/acs.jpcc.0c07920.

Modeling of visible triplet absorption kinetics, modeling of triplet population dynamics from ultrafast vibrational spectra, demonstration of no thermal annealing of amorphous samples during TA spectroscopy measurements (PDF)

AUTHOR INFORMATION

Corresponding Author

John B. Asbury − *Department of Chemistry and Intercollege Materials Science and Engineering Program, The Pennsylvania State University, University Park, Pennsylvania 16801, United States;* orcid.org/0000-0002-3641-7276; Email: jasbury@psu.edu

Authors

Kyle T. Munson − *Department of Chemistry, The Pennsylvania State University, University Park, Pennsylvania 16801, United States*

Jianing Gan − *Department of Chemistry, The Pennsylvania State University, University Park, Pennsylvania 16801, United States*

Christopher Grieco − *Department of Chemistry, The Pennsylvania State University, University Park, Pennsylvania 16801, United States*

Grayson S. Doucette − *Intercollege Materials Science and Engineering Program, The Pennsylvania State University, University Park, Pennsylvania 16801, United States*

John E. Anthony − *Department of Chemistry, University of Kentucky, Lexington, Kentucky 40506, United States;* orcid.org/0000-0002-8972-1888

Complete contact information is available at: https://pubs.acs.org/10.1021/acs.jpcc.0c07920

Notes

The authors declare the following competing financial interest(s): C.G. and J.B.A. own equity in Magnitude Instruments, which has an interest in this project. Their ownership in this company has been reviewed by the Pennsylvania State University's Individual Conflict of Interest Committee and is currently being managed by the University.

ACKNOWLEDGMENTS

J.G., C.G., G.S.D., and J.B.A. thank the U.S. Department of Energy (DOE), Office of Science, Office of Basic Energy Sciences for support of this research through Grant DE-SC0019349. K.T.M. is grateful for support from the National

Science Foundation Graduate Research Fellowship Program under Grant DGE-1255832. Any opinions, findings, and conclusions or recommendations expressed in this material are those of the author(s) and do not necessarily reflect the views of the National Science Foundation. Organic semiconductor synthesis (J.E.A.) was supported by the National Science Foundation under Cooperative Agreement No. 1849213.

REFERENCES

(1) Smith, M. B.; Michl, J. Singlet Fission. *Chem. Rev.* **2010**, *110*, 6891−6936.
(2) Kasai, Y.; Tamai, Y.; Ohkita, H.; Benten, H.; Ito, S. Ultrafast Singlet Fission in a Push-Pull Low-Bandgap Polymer Film. *J. Am. Chem. Soc.* **2015**, *137*, 15980−15983.
(3) Musser, A. J.; Al-Hashimi, M.; Maiuri, M.; Brida, D.; Heeney, M.; Cerullo, G.; Friend, R. H.; Clark, J. Activated Singlet Exciton Fission in a Semiconducting Polymer. *J. Am. Chem. Soc.* **2013**, *135*, 12747−12754.
(4) Pensack, R. D.; Ostroumov, E. E.; Tilley, A. J.; Mazza, S.; Grieco, C.; Thorley, K. J.; Asbury, J. B.; Seferos, D. S.; Anthony, J. E.; Scholes, G. D. Observation of Two Triplet-Pair Intermediates in Singlet Exciton Fission. *J. Phys. Chem. Lett.* **2016**, *7*, 2370−2375.
(5) Grieco, C.; Kennehan, E. R.; Kim, H.; Pensack, R. D.; Brigeman, A. N.; Rimshaw, A.; Payne, M. M.; Anthony, J. E.; Giebink, N. C.; Scholes, G. D.; et al. Direct Observation of Correlated Triplet Pair Dynamics During Singlet Fission Using Ultrafast Mid-Ir Spectroscopy. *J. Phys. Chem. C* **2018**, *122*, 2012−2022.
(6) Pensack, R. D.; Tilley, A. J.; Grieco, C.; Purdum, G. E.; Ostroumov, E. E.; Granger, D. B.; Oblinsky, D. G.; Dean, J. C.; Doucette, G. S.; Asbury, J. B.; et al. Striking the Right Balance of Intermolecular Coupling for High-Efficiency Singlet Fission. *Chem. Sci.* **2018**, *9*, 6240−6259.
(7) Yost, S. R.; Lee, J.; Wilson, M. W.; Wu, T.; McMahon, D. P.; Parkhurst, R. R.; Thompson, N. J.; Congreve, D. N.; Rao, A.; Johnson, K.; et al. A Transferable Model for Singlet-Fission Kinetics. *Nat. Chem.* **2014**, *6*, 492−497.
(8) Wilson, M. W.; Rao, A.; Clark, J.; Kumar, R. S.; Brida, D.; Cerullo, G.; Friend, R. H. Ultrafast Dynamics of Exciton Fission in Polycrystalline Pentacene. *J. Am. Chem. Soc.* **2011**, *133*, 11830−11833.
(9) Musser, A. J.; Liebel, M.; Schnedermann, C.; Wende, T.; Kehoe, T. B.; Rao, A.; Kukura, P. Evidence for Conical Intersection Dynamics Mediating Ultrafast Singlet Exciton Fission. *Nat. Phys.* **2015**, *11*, 352−357.
(10) Pensack, R. D.; Grieco, C.; Purdum, G. E.; Mazza, S. M.; Tilley, A. J.; Ostroumov, E. E.; Seferos, D. S.; Loo, Y.-L.; Asbury, J. B.; Anthony, J. E.; et al. Solution-Processable, Crystalline Material for Quantitative Singlet Fission. *Mater. Horiz.* **2017**, *4*, 915−923.
(11) Grieco, C.; Kennehan, E. R.; Rimshaw, A.; Payne, M. M.; Anthony, J. E.; Asbury, J. B. Harnessing Molecular Vibrations to Probe Triplet Dynamics During Singlet Fission. *J. Phys. Chem. Lett.* **2017**, *8*, 5700−5706.
(12) Breen, I.; Tempelaar, R.; Bizimana, L. A.; Kloss, B.; Reichman, D. R.; Turner, D. B. Triplet Separation Drives Singlet Fission after Femtosecond Correlated Triplet Pair Production in Rubrene. *J. Am. Chem. Soc.* **2017**, *139*, 11745−11751.
(13) Roberts, S. T.; McAnally, R. E.; Mastron, J. N.; Webber, D. H.; Whited, M. T.; Brutchey, R. L.; Thompson, M. E.; Bradforth, S. E. Efficient Singlet Fission Discovered in a Disordered Acene Film. *J. Am. Chem. Soc.* **2012**, *134*, 6388−400.
(14) Monahan, N. R.; Sun, D.; Tamura, H.; Williams, K. W.; Xu, B.; Zhong, Y.; Kumar, B.; Nuckolls, C.; Harutyunyan, A. R.; Chen, G.; et al. Dynamics of the Triplet-Pair State Reveals the Likely Coexistence of Coherent and Incoherent Singlet Fission in Crystalline Hexacene. *Nat. Chem.* **2017**, *9*, 341−346.
(15) Scholes, G. D. Correlated Pair States Formed by Singlet Fission and Exciton-Exciton Annihilation. *J. Phys. Chem. A* **2015**, *119*, 12699−12705.
(16) Zurek, W. H. Decoherence and the Transition from Quantum to Classical. *Phys. Today* **1991**, *44*, 36−44.
(17) Yang, L.; Tabachnyk, M.; Bayliss, S. L.; Böhm, M. L.; Broch, K.; Greenham, N. C.; Friend, R. H.; Ehrler, B. Solution-Processable Singlet Fission Photovoltaic Devices. *Nano Lett.* **2015**, *15*, 354−358.
(18) Tabachnyk, M.; Ehrler, B.; Bayliss, S.; Friend, R. H.; Greenham, N. C. Triplet Diffusion in Singlet Exciton Fission Sensitized Pentacene Solar Cells. *Appl. Phys. Lett.* **2013**, *103*, 153302.
(19) Reusswig, P. D.; Congreve, D. N.; Thompson, N. J.; Baldo, M. A. Enhanced External Quatum Efficiency in an Organic Photovoltaic Cell Via Singlet Fission Exciton Sensitizer. *Appl. Phys. Lett.* **2012**, *101*, 113304.
(20) Poletayev, A. D.; Clark, J.; Wilson, M. W.; Rao, A.; Makino, Y.; Hotta, S.; Friend, R. H. Triplet Dynamics in Pentacene Crystals: Applications to Fission-Sensitized Photovoltaics. *Adv. Mater.* **2014**, *26*, 919−924.
(21) Shockley, W.; Queisser, H. J. Detailed Balance Limit of Efficiency of P-N Junction Solar Cells. *J. Appl. Phys.* **1961**, *32*, 510−519.
(22) Broch, K.; Dieterle, J.; Branchi, F.; Hestand, N. J.; Olivier, Y.; Tamura, H.; Cruz, C.; Nichols, V. M.; Hinderhofer, A.; Beljonne, D.; Spano, F. C.; Cerullo, G.; Bardeen, C. J.; Schreiber, F. Robust Singlet Fission in Pentacene Thin Films with Tuned Charge Transfer Interactions. *Nat. Commun.* **2018**, *9*, 954.
(23) Piland, G. B.; Burdett, J. J.; Dillon, R. J.; Bardeen, C. J. Singlet Fission: From Coherences to Kinetics. *J. Phys. Chem. Lett.* **2014**, *5*, 2312−2319.
(24) Walker, B. J.; Musser, A. J.; Beljonne, D.; Friend, R. H. Singlet Exciton Fission in Solution. *Nat. Chem.* **2013**, *5*, 1019−1024.
(25) Sanders, S. N.; Kumarasamy, E.; Pun, A. B.; Trinh, M. T.; Choi, B.; Xia, J.; Taffet, E. J.; Low, J. Z.; Miller, J. R.; Roy, X.; Zhu, X.-Y.; Steigerwald, M. L.; Sfeir, M. Y.; Campos, L. M. Quantitative Intramolecular Singlet Fission in Bipentacenes. *J. Am. Chem. Soc.* **2015**, *137*, 8965−8972.
(26) Casillas, R.; Papadopoulos, I.; Ullrich, T.; Thiel, D.; Kunzmann, A.; Guldi, D. M. Molecular Insights and Concepts to Engineer Singlet Fission Energy Conversion Devices. *Energy Environ. Sci.* **2020**, *13*, 2741−2804.
(27) Allardice, J. R.; Thampi, A.; Dowland, S.; Xiao, J.; Gray, V.; Zhang, Z.; Budden, P.; Petty, A. J. I.; Davis, N. J. L. K.; Greenham, N. C.; et al. Engineering Molecular Ligand Shells on Quantum Dots for Quantitative Harvesting of Triplet Excitons Generated by Singlet Fission. *J. Am. Chem. Soc.* **2019**, *141*, 12907−12915.
(28) Einzinger, M.; Wu, T.; Kompalla, J. F.; Smith, H. L.; Perkinson, C. F.; Nienhaus, L.; Wieghold, S.; Congreve, D. N.; Kahn, A.; Bawendi, M. G.; et al. Sensitization of Silicon by Singlet Exciton Fission in Tetracene. *Nature* **2019**, *571*, 90−94.
(29) MacQueen, R. W.; Liebhaber, M.; Niederhausen, J.; Mews, M.; Gersmann, C.; Jäckle, S.; Jager, K.; Tayebjee, M. J. Y.; Schmidt, T. W.; Rech, B.; Lips, K. Crystalline Silicon Solar Cells with Tetracene Interlayers: The Path to Silicon-Singlet Fission Heterojunction Devices. *Mater. Horiz.* **2018**, *5*, 1065−1075.
(30) Pace, N. A.; Korovina, N.; Clikeman, T. T.; Holliday, S.; Granger, D. B.; Carroll, G. M.; Nanayakkara, S. U.; Anthony, J. E.; McCulloch, I.; Strauss, S. H.; et al. Slow Charge Transfer from Pentacene Triplet States at the Marcus Optimum. *Nat. Chem.* **2020**, *12*, 63−70.
(31) Grieco, C.; Doucette, G. S.; Munro, J. M.; Kennehan, E. R.; Lee, Y.; Rimshaw, A.; Payne, M. M.; Wonderling, N.; Anthony, J. E.; Dabo, I.; et al. Triplet Transfer Mediates Triplet Pair Separation During Singlet Fission in 6,13-Bis(Triisopropylsilylethynyl)-Pentacene. *Adv. Funct. Mater.* **2017**, *27*, 1703929.
(32) Lee, T. S.; Lin, Y. L.; Kim, H.; Rand, B. P.; Scholes, G. D. Two Temperature Regimes of Triplet Transfer in the Dissociation of the Correlated Triplet Pair after Singlet Fission. *Can. J. Chem.* **2019**, *97*, 465−473.

https://dx.doi.org/10.1021/acs.jpcc.0c07920
J. Phys. Chem. C 2020, 124, 23567−23578

(33) Lee, T. S.; Lin, Y. L.; Kim, H.; Pensack, R. D.; Rand, B. P.; Scholes, G. D. Triplet Energy Transfer Governs the Dissociation of the Correlated Triplet Pair in Exothermic Singlet Fission. *J. Phys. Chem. Lett.* **2018**, *9*, 4087−4095.
(34) Mirkovic, T.; Ostroumov, E. E.; Anna, J. M.; van Grondelle, R.; Govindjee; Scholes, G. D. Light Absorption and Energy Transfer in the Antenna Complexes of Photosynthetic Organisms. *Chem. Rev.* **2017**, *117*, 249−293.
(35) Doucette, G. S.; Huang, H.-T.; Munro, J. M.; Munson, K. T.; Park, C.; Anthony, J. E.; Strobel, T.; Dabo, I.; Badding, J. V.; Asbury, J. B. Tuning Triplet-Pair Separation Versus Relaxation Using a Diamond Anvil Cell. *Cell Rep. Phys. Sci.* **2020**, *1*, 100005.
(36) Busby, E.; Xia, J.; Wu, Q.; Low, J. Z.; Song, R.; Miller, J. R.; Zhu, X. Y.; Campos, L. M.; Sfeir, M. Y. A Design Strategy for Intramolecular Singlet Fission Mediated by Charge-Transfer States in Donor-Acceptor Organic Materials. *Nat. Mater.* **2015**, *14*, 426−433.
(37) Zhai, Y.; Sheng, C.; Vardeny, Z. V. Singlet Fission of Hot Excitons in Pi-Conjugated Polymers. *Philos. Trans. R. Soc., A* **2015**, *373*, 20140327.
(38) Musser, A. J.; Al-Hashimi, M.; Heeney, M.; Clark, J. Heavy-Atom Effects on Intramolecular Singlet Fission in a Conjugated Polymer. *J. Chem. Phys.* **2019**, *151*, 044902.
(39) Pace, N. A.; Zhang, W.; Arias, D. H.; McCulloch, A.; Rumbles, G.; Johnson, J. C. Controlling Long-Lived Triplet Generation from Intramolecular Singlet Fission in the Solid State. *J. Phys. Chem. Lett.* **2017**, *8*, 6086−6091.
(40) Bange, S.; Scherf, U.; Lupton, J. M. Absence of Singlet Fission and Carrier Multiplication in a Model Conjugated Polymer: Tracking the Triplet Population through Photophorescence. *J. Am. Chem. Soc.* **2012**, *134*, 1946−1949.
(41) Hu, J.; Xu, K.; Shen, L.; Wu, Q.; He, G.; Wang, J.-Y.; Pei, J.; Xia, J.; Sfeir, M. Y. New Insights into the Design of Conjugated Polymers for Intramolecular Singlet Fission. *Nat. Commun.* **2018**, *9*, 2999.
(42) Richardson, M. J. Crystallinity Determination in Polymers and a Quantitative Comparison for Polyethylene. *Br. Polym. J.* **1969**, *1*, 132−137.
(43) Grieco, C.; Doucette, G. S.; Pensack, R. D.; Payne, M. M.; Rimshaw, A.; Scholes, G. D.; Anthony, J. E.; Asbury, J. B. Dynamic Exchange During Triplet Transport in Nanocrystalline Tips-Pentacene Films. *J. Am. Chem. Soc.* **2016**, *138*, 16069−16080.
(44) Margulies, E. A.; Wu, Y.-L.; Gawel, P.; Miller, S. A.; Shoer, L. E.; Schaller, R. D.; Diederich, F.; Wasielewski. Sub-Picosecond Singlet Exciton Fission in Cyano-Substituted Diaryltetracenes. *Angew. Chem., Int. Ed.* **2015**, *54*, 8679−8683.
(45) Arias, D. H.; Ryerson, J. L.; Cook, J. D.; Damrauer, N. H.; Johnson, J. C. Polymorphism Influences Singlet Fission Rates in Tetracene Thin Films. *Chem. Sci.* **2016**, *7*, 1185−1191.
(46) Hartnett, P. E.; Margulies, E. A.; Mauck, C. M.; Miller, S. A.; Wu, Y.; Wu, Y. L.; Marks, T. J.; Wasielewski, M. R. Effects of Crystal Morphology on Singlet Exciton Fission in Diketopyrrolopyrrole Thin Films. *J. Phys. Chem. B* **2016**, *120*, 1357−1366.
(47) Sharifzadeh, S.; Wong, C. Y.; Wu, H.; Cotts, B. L.; Kronik, L.; Ginsberg, N. S.; Neaton, J. B. Relating the Physical Structure and Optoelectronic Function of Crystalline Tips-Pentacene. *Adv. Funct. Mater.* **2015**, *25*, 2038−2046.
(48) Pensack, R. D.; Tilley, A. J.; Parkin, S. R.; Lee, T. S.; Payne, M. M.; Gao, D.; Jahnke, A. A.; Oblinsky, D. G.; Li, P. F.; Anthony, J. E.; et al. Exciton Delocalization Drives Rapid Singlet Fission in Nanoparticles of Acene Derivatives. *J. Am. Chem. Soc.* **2015**, *137*, 6790−6803.
(49) Grieco, C.; Doucette, G. S.; Munson, K. T.; Swartzfager, J. R.; Munro, J. M.; Anthony, J. E.; Dabo, I.; Asbury, J. B. Vibrational Probe of the Origin of Singlet Exciton Fission in Tips-Pentacene Solutions. *J. Chem. Phys.* **2019**, *151*, 154701.
(50) Barbour, L. W.; Hegadorn, M.; Asbury, J. B. Watching Electrons Move in Real Time: Ultrafast Infrared Spectroscopy of a Polymer Blend Photovoltaic Material. *J. Am. Chem. Soc.* **2007**, *129*, 15884−15894.
(51) Diao, Y.; Lenn, K. M.; Lee, W.-Y.; Blood-Forsythe, M. A.; Xu, J.; Mao, Y.; Kim, Y.; Reinspach, J. A.; Park, S.; Aspuru-Guzik, A.; et al. Understanding Polymorphism in Organic Semiconductor Thin Films through Nanoconfinement. *J. Am. Chem. Soc.* **2014**, *136*, 17046−17057.
(52) Smith, M. B.; Michl, J. Recent Advances in Singlet Fission. *Annu. Rev. Phys. Chem.* **2013**, *64*, 361−386.
(53) Ramanan, C.; Smeigh, A. L.; Anthony, J. E.; Marks, T. J.; Wasielewski, M. R. Competition between Singlet Fission and Charge Separation in Solution-Processed Blend Films of 6,13-Bis-(Triisopropylsilylethynyl)Pentacene with Sterically-Encumbered Perylene-3,4:9,10-Bis(Dicarboximide)S. *J. Am. Chem. Soc.* **2012**, *134*, 386−397.
(54) Margulies, E. A.; Kerisit, N.; Gawel, P.; Mauck, C. M.; Ma, L.; Miller, C. E.; Young, R. M.; Trapp, N.; Wu, Y.-L.; Diederich, F.; et al. Substituent Effects on Singlet Exciton Fission in Polycrystalline Thin Films of Cyano-Substituted Diaryltetracenes. *J. Phys. Chem. C* **2017**, *121*, 21262−21271.
(55) Dereka, B.; Svechkarev, D.; Rosspeintner, A.; Tromayer, M.; Liska, R.; Mohs, A. M.; Vauthey, E. Direct Observation of a Photochemical Alkyne−Allene Reaction and of a Twisted and Rehybridized Intramolecular Charge-Transfer State in a Donor−Acceptor Dyad. *J. Am. Chem. Soc.* **2017**, *139*, 16885−16893.
(56) Kennehan, E. R.; Grieco, C.; Brigeman, A. N.; Doucette, G. S.; Rimshaw, A.; Bisgaier, K.; Giebink, N. C.; Asbury, J. B. Using Molecular Vibrations to Probe Exciton Delocalization in Films of Perylene Diimides with Ultrafast Mid-Ir Spectroscopy. *Phys. Chem. Chem. Phys.* **2017**, *19*, 24829−24839.
(57) Kennehan, E. R.; Munson, K. T.; Doucette, G. S.; Marshall, A. R.; Beard, M. C.; Asbury, J. B. Dynamic Ligand Surface Chemistry of Excited Pbs Quantum Dots. *J. Phys. Chem. Lett.* **2020**, *11*, 2291−2297.
(58) Taylor, V. C. A.; Tiwari, D.; Duchi, M.; Donaldson, P. M.; Clark, I. P.; Fermin, D. J.; Oliver, T. A. A. Investigating the Role of the Organic Cation in Formamidinium Lead Iodide Perovskite Using Ultrafast Spectroscopy. *J. Phys. Chem. Lett.* **2018**, *9*, 895−901.
(59) Munson, K. T.; Doucette, G. S.; Kennehan, E. R.; Swartzfager, J. R.; Asbury, J. B. Vibrational Probe of the Structural Origins of Slow Recombination in Halide Perovskites. *J. Phys. Chem. C* **2019**, *123*, 7061−7073.
(60) Lin, J. D. A.; Mikhnenko, O. V.; Chen, J.; Masri, Z.; Ruseckas, A.; Mikhailovsky, A.; Raab, R. P.; Liu, J.; Blom, P. W. M.; Loi, M. A.; et al. Systematic Study of Exciton Diffusion Length in Organic Semiconductor by Six Experimental Methods. *Mater. Horiz.* **2014**, *1*, 280−285.
(61) Zhang, Y.; Forrest, S. R. Triplet Diffusion Leads to Triplet−Triplet Annihilation in Organic Phosphorescent Emitters. *Chem. Phys. Lett.* **2013**, *590*, 106−110.

https://dx.doi.org/10.1021/acs.jpcc.0c07920
J. Phys. Chem. C 2020, 124, 23567−23578